

***p*-*sd* Shell Gap Reduction in Neutron-Rich Systems and Cross-Shell Excitations in  $^{20}\text{O}$** 

M. Wiedeking, S. L. Tabor, J. Pavan, A. Volya, A. L. Aguilar, I. J. Calderin, D. B. Campbell, W. T. Cluff, E. Diffenderfer, J. Fridmann, C. R. Hoffman, K. W. Kemper, S. Lee, M. A. Riley, B. T. Roeder, C. Teal, V. Tripathi, and I. Wiedenhöver

*Florida State University, Tallahassee, Florida 32306, USA*

(Received 13 December 2004; published 7 April 2005)

Excited states in  $^{20}\text{O}$  were populated in the reaction  $^{10}\text{Be}(^{14}\text{C}, \alpha)$  at Florida State University (FSU). Charged particles were detected with a particle telescope consisting of 4 annularly segmented Si surface barrier detectors and  $\gamma$  radiation was detected with the FSU  $\gamma$  detector array. Five new states were observed below 6 MeV from the  $\alpha$ - $\gamma$  and  $\alpha$ - $\gamma$ - $\gamma$  coincidence data. Shell model calculations suggest that most of the newly observed states are core-excited  $1p$ - $1h$  excitations across the  $N = Z = 8$  shell gap. Comparisons between experimental data and calculations for the neutron-rich O and F isotopes imply a steady reduction of the *p*-*sd* shell gap as neutrons are added.

DOI: 10.1103/PhysRevLett.94.132501

PACS numbers: 23.20.Lv, 21.60.Cs, 25.60-t, 27.30.+t

The mean field is a central concept in all macroscopic many-body phenomena; in nuclei it leads to shell structure and magic numbers and it provides the basis for the most powerful theoretical techniques such as the nuclear shell model. In recent years attention has been focused on light nuclei, which are intermediate between macroscopic and few-body nucleonic systems, because they can exhibit extreme modifications or even a complete breakdown of the mean-field approach. This behavior emphasizes the underlying question of nature of how combinations of a few simple building blocks can lead to the astonishing diversity and complexity of many-body phenomena. Interest in this subject is fueled by experimental advances which allow for the exploration of nuclear structure at the limit of stability with extreme proton to neutron ratios.

The most significant manifestation of shell breaking is seen in nearly semimagic nuclei, where the mean-field shell structure breaks down as a function of the proton to neutron ratio. The “island of inversion” [1] has been observed around the neutron shell closure at  $N = 20$  [2] where the mean-field shell structure is weakened due to the proton-neutron imbalance and residual interactions dominate [3,4]. This modification of the shell structure leads to configurations where intruders dominate low-lying states.

An analogous situation appears one shell below, in the  $Z = 2$  He isotopes, where the intrusion of *sd* excitations in *p*-shell configurations becomes important in the heavy helium isotopes. Although the neutron drip line at  $^8\text{He}$  is reached before inversion, the resonant states exhibit significant fragmentation of the single-particle decay strength due to *sd*-shell intruder configurations [5]. It is still controversial if the lowest energy resonance corresponding to unbound  $^9\text{He}$  is an inverted structure with an odd particle in the *sd* shell and thus of positive parity. The intruder ground state in  $^{11}\text{Be}$  [6] is another example of a weakened shell gap.

The oxygen isotopes, which lie at the  $Z = 8$  shell boundary, provide an excellent opportunity to investigate

the effects of neutron excess on the shell gap and cross-shell excitations. Possible modifications of the shell structure with neutron excess raise important questions related to the surprisingly large shift in the neutron drip line between the O and F isotopes [7,8]. Cross-shell *p*-*sd* excitations are known to be essential in the structure of nuclei in this region, such as the 110 keV  $1^-$  state in  $^{19}\text{F}$  [9].

The availability of suitable reactions has limited the study of the neutron-rich O isotopes. Most of the previous work on  $^{20}\text{O}$  has involved one of the earliest radioactive beams through the  $^{18}\text{O}(t, p)$  reaction [10–12]. Fragmentation reactions were recently used to determine  $\gamma$  decays from some previously known states [13]. Intruder states, which have an odd number of nucleons promoted across the *p*-*sd* shell gap, provide the clearest evidence for cross-shell excitations. Only 2 intruder states, a  $1^-$  at 5.35(10) MeV [14] and a tentative ( $3^-$ ) at 5.614(3) MeV [15,16], had been identified in  $^{20}\text{O}$  prior to the present work. However, shell model calculations including *p* shell excitations predict significantly more states in the region of 4.5 to 6 MeV. Because of this discrepancy the present experiment was performed to study the shell structure of  $^{20}\text{O}$ .

In this Letter, we report on the addition of five new states in  $^{20}\text{O}$  below an excitation energy of 6 MeV. With the additional experimental information, shell model calculations were performed for neutron-rich O and F isotopes. These provide strong evidence for a reduction of the *p*-*sd* shell gap as neutrons are added.

To populate  $^{20}\text{O}$ , a long-lived radioactive beam and target were employed through the  $^{10}\text{Be}(^{14}\text{C}, \alpha)$  reaction at 21.4 MeV. The  $^{14}\text{C}$  beam was provided by the Florida State University (FSU) Superconducting Accelerator Laboratory. The  $113 \mu\text{g}/\text{cm}^2$   $^{10}\text{Be}$  target on a  $1 \text{ mg}/\text{cm}^2$  thick Pt backing was specially made [17]. Neutron evaporation dominated the reaction, and  $^{20}\text{O}$  could be observed only by detecting the  $\alpha$  particles. These were detected in an  $E$ - $\Delta E$  Si telescope, consisting of a  $150 \mu\text{m}$   $\Delta E$  detector and a stack of three  $1500 \mu\text{m}$   $E$  detectors. All four Si

wafers were divided into 4 annular segments and placed at  $0^\circ$  relative to the beam. A  $32 \text{ mg/cm}^2$  thick gold foil was placed between the target and detector telescope to stop the beam.  $\gamma$  radiation was detected in coincidence with the  $\alpha$  particles using the FSU Compton suppressed  $\gamma$ -detector array. During the experiment  $4.3 \times 10^6$   $\alpha$ - $\gamma$  events were recorded.

The data were analyzed using GNUSCOPE [18]. The  $\alpha$  spectra from the 4 annular segments were kinematically corrected, and a Doppler correction was applied to the  $\gamma$  spectra. Although the target contained significant amounts of  $^{16}\text{O}$  and  $^{12}\text{C}$ , the corresponding reaction products,  $^{26}\text{Mg}$  and  $^{22}\text{Ne}$ , are well-known and their lines were removed from consideration.

A portion of the  $\alpha$ - $\gamma$  spectrum in coincidence with the lowest  $2_1^+ \rightarrow 0_1^+$  transition at 1674 keV is shown in Fig. 1. The  $\alpha$ - $\gamma$  coincidences with most of the newly assigned lines are shown in Fig. 2. Clear coincidences with the 1674 keV transition ( $2_1^+ \rightarrow 0_1^+$ ) can be seen in all these spectra. Placement of the  $\gamma$  transitions was verified by the coincident  $\alpha$  energies, as described in Ref. [19]. Examples of  $\alpha$  spectra obtained by gating on  $\gamma$  lines are shown in Fig. 3 to illustrate how the placement of the new lines fits with the  $\alpha$  spectra of the known lines. The level scheme from this and previous work is shown in Fig. 4. The uncertainties in  $\gamma$ -ray energies range from 1 keV up to 6 keV for the weaker new transitions.

Although the 5 new states at 3895, 4353, 4598, 5115, and 5873 keV have not been previously reported, a careful examination of previous studies of  $^{20}\text{O}$  does reveal hints of their existence. Very small peaks are visible in the  $^{18}\text{O}(t, p)$

spectrum shown in Fig. 1 of Ref. [15] at 3.9, 4.6, 5.1, and possibly 5.9 MeV. While examination of only one spectrum at one angle cannot rule out contaminants, the weakness of these peaks is consistent with their weak population in the present experiment. Interestingly, a tentative state was reported at 5.83(20) MeV in an early paper [20] and included in an earlier compilation [21]. A state was reported at 6.02 MeV in another measurement [10]. The 5.83 MeV state was dropped from the subsequent compilation [22], possibly because it was not confirmed in Ref. [15]. The state observed here at 5873 keV may correspond to one or both of these previously reported states.

While shell model calculations restricted to the  $p$  shell or to the  $sd$  shell have been very successful in describing the structure of nuclei in these regions, the description of excitations between the  $p$  and  $sd$  shells has been much more limited. The lack of experimental data and increased dimensionality of such calculations together with the center-of-mass issue [23] resulted in the lack of well tested interactions. To gain an understanding of the current experimental results,  $p$ - $sd$  shell model calculations were performed for neutron-rich O and F isotopes using and slightly modifying (as discussed below) cross-shell interactions from Refs. [1,24]. Calculations were also conducted taking excitations into the  $fp$  shell into account.

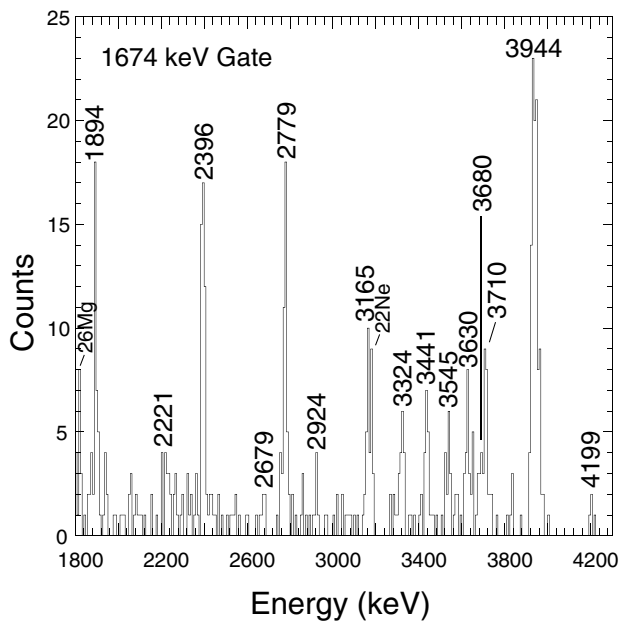


FIG. 1. Transitions in coincidence with  $\alpha$  particles and the 1674 keV  $\gamma$  ray ( $2_1^+ \rightarrow 0_1^+$ ). The lines in this spectrum marked by their energies correspond to decays in  $^{20}\text{O}$ .

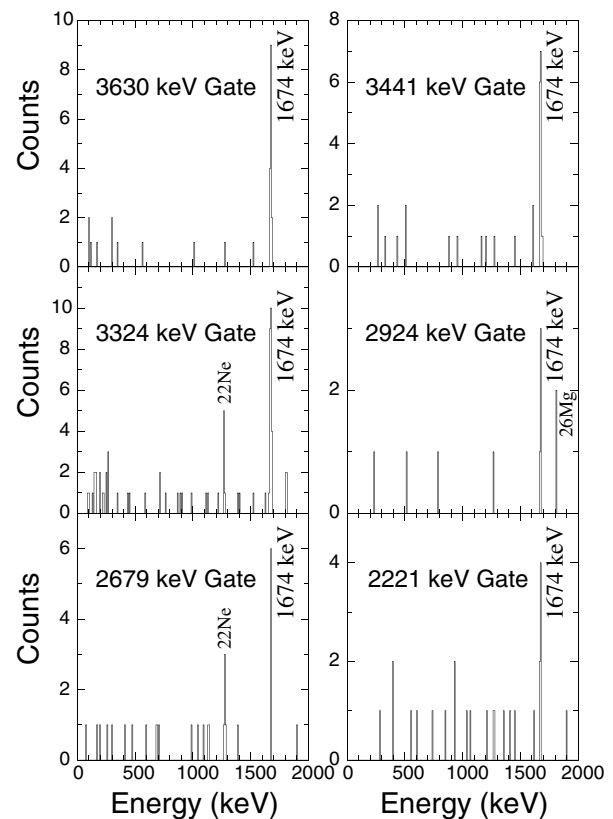


FIG. 2. Spectra in coincidence with  $\alpha$  particles and newly observed transitions in  $^{20}\text{O}$ .

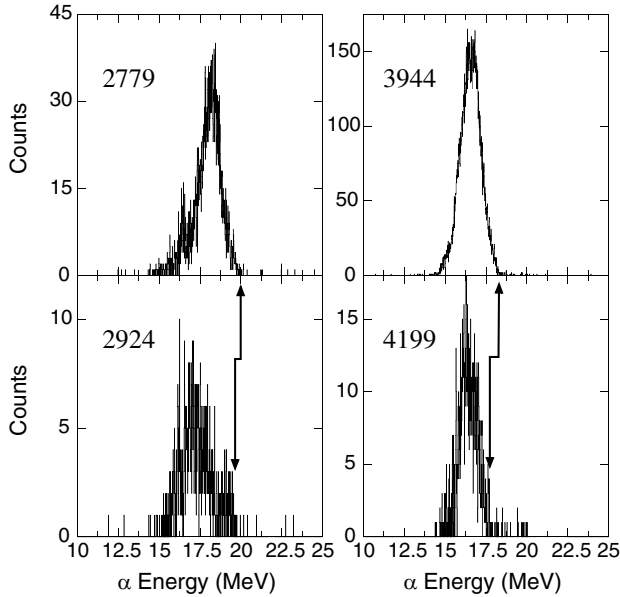


FIG. 3.  $\alpha$  spectra for two  $\gamma$ -ray pairs originating from states with similar excitation energies. The spectra are labeled by their energy (in keV) of the  $\gamma$ -ray gate.

However, at excitation energies of interest  $fp$  configurations proved to be of no importance.

For the calculations, an  $m$ -scheme shell model code developed at FSU [25] was used which allows for a full diagonalization of the  $p$ - $sd$  shell simultaneously. However, the interactions based on a perturbative merging of the  $sd$  and  $p$  shells imply a particle-hole hierarchy. Establishing a trend in reproducing the experimental data is a key step in

validating the model calculations. The monopole corrected single-particle energies in the  $sd$  shell were adjusted to reproduce single-nucleon excitations in  $^{17}\text{O}$ . Thus, the model is in good agreement with universal  $sd$  (USD) shell model results. The cross-shell excitations in  $^{16}\text{O}$  are also well reproduced. The perturbative combined  $p$ - $sd$  shell model essentially has one parameter, the shell gap. The role of this gap becomes more essential in establishing the relative positions of cross-shell excitations as the neutron number  $N$  increases above the shell closure at  $N = 8$ . Considering negative-parity states in  $^{18,19,20,22}\text{O}$  and using the original interaction, a significant trend of deviation is found. For example, the  $1p$ - $1h$  states in  $^{22}\text{O}$  are predicted to be more than 1 MeV above the first tentatively observed negative-parity state at 5.8 MeV [26]. The agreement with experimentally observed states can be improved significantly by reducing the  $p$ - $sd$  shell gap with increasing neutron number. The necessity to reduce the shell gap to obtain the best agreement between experimental and theoretical states is also observed in the neutron-rich  $^{19,20,22}\text{F}$  isotopes. This suggests a general  $p$ - $sd$  shell gap decrease as more neutrons are added, in agreement with theoretical predictions [27]. The reduction in the effective single-particle energy as a function of nucleon number for neutron-rich O and F isotopes is shown in Fig. 5. The diminishing of the shell gap emphasizes the approach to a region of intruder dominated structures.

The agreement in energy with experimentally observed states in  $^{20}\text{O}$  can be improved significantly by reducing the  $p$ - $sd$  shell gap by 850 keV. Figure 6 compares the calculated and experimentally observed states in  $^{18}\text{O}$  and  $^{20}\text{O}$ , where the closed shell  $^{16}\text{O}$  single-particle energies are used

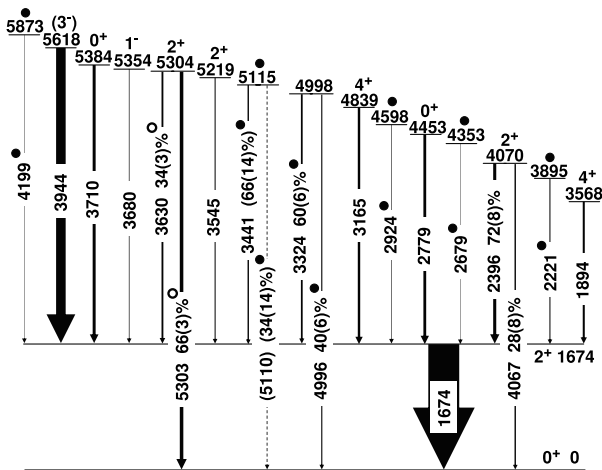


FIG. 4. The level scheme as deduced from current and previous work. The widths of the lines indicate their intensities normalized to the 1674 keV transition. Branching ratios are given where applicable. States and transitions marked with solid circles are new additions.  $\gamma$  transitions with open circles were tentatively reported in Ref. [12] and are confirmed in the present work.

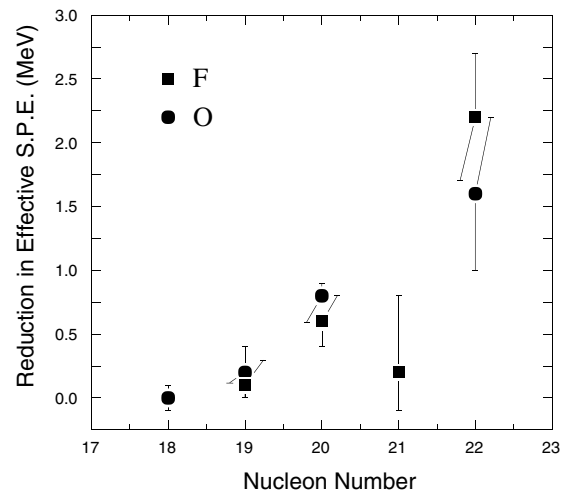


FIG. 5. Systematic reduction of the  $p$ - $sd$  shell gap as neutrons are added to O and F nuclei. Shell model calculations were performed and the shell gap adjusted based on the comparison to available experimental data from the current work and Refs. [18,26,28]. The error bars reflect the current experimental knowledge available for the respective nuclei.

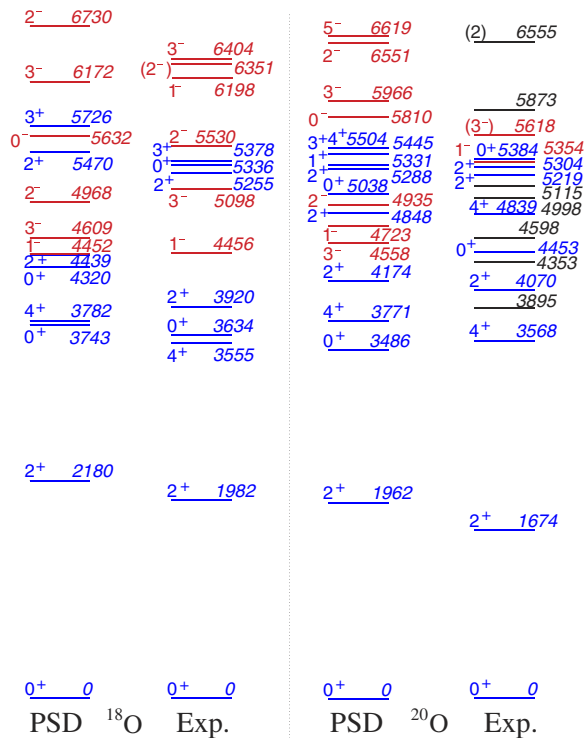


FIG. 6 (color online). Comparison of calculated and experimentally observed states in  $^{18}\text{O}$  and  $^{20}\text{O}$ . States in blue indicate positive-parity states ( $0p-0h$  and  $2p-2h$ ); states in red are negative-parity states ( $1p-1h$ ). The levels in black at 3895, 4353, 4598, 5115, and 5873 keV are new additions in  $^{20}\text{O}$ . Also shown in black is the previously known 6555 keV state where no parity assignment is available. For  $^{18}\text{O}$  the standard  $^{16}\text{O}$  closed shell single-particle energies are used, whereas for  $^{20}\text{O}$  the  $p$ - $sd$  shell gap was reduced by 850 keV.

for  $^{18}\text{O}$  and a reduced  $p$ - $sd$  shell gap of 850 keV is used for  $^{20}\text{O}$ . The theoretical states shown in blue are mainly the pure  $sd$  ones involving only valence neutrons outside the closed  $^{16}\text{O}$  core using the USD interaction. Two states at 3743 and 5470 keV in  $^{18}\text{O}$  and at 3486 and 4848 keV in  $^{20}\text{O}$  are due to  $2p-2h$  excitations. Previously known experimental positive-parity states are also shown in blue. There is good agreement in the energies of the positive-parity states in  $^{18}\text{O}$  and  $^{20}\text{O}$ . The tendency to overpredict the energy of the first  $2^+$  state is somewhat greater in  $^{20}\text{O}$ . Negative-parity  $1p-1h$  states (red) are predicted to start at about 4.5 MeV in both nuclei. There are good candidates in  $^{18}\text{O}$  within a few hundred keV for all but one of the predicted negative-parity states. In  $^{20}\text{O}$  the lowest previously established negative-parity state lies about 800 keV above the first predicted one. However, some of the newly observed levels lie reasonably close to a number of the predicted negative-parity states. Unfortunately, the newly observed states are populated too weakly to determine their

spins or parities, but there is a good qualitative agreement between experiment and theory in  $^{20}\text{O}$  with the addition of the new states.

To conclude, in this work we report five new states that were observed in semimagic  $^{20}\text{O}$  below 6 MeV through the measurement of  $\alpha$ - $\gamma$  and  $\alpha$ - $\gamma$ - $\gamma$  coincidences following population in the  $^{10}\text{Be}(^{14}\text{C}, \alpha)$  reaction using a long-lived radioactive  $^{14}\text{C}$  beam and a specially prepared radioactive  $^{10}\text{Be}$  target. Many of the newly observed levels appear to be the predicted core-excited  $1p-1h$  negative-parity states. Comparison between shell model calculations and experimental observation of neutron-rich O and F isotopes implies a systematic reduction in the effective  $p$ - $sd$  shell gap, indicating a weakening of the gap as neutrons are added.

This work was supported in part by the U.S. National Science Foundation under Grant No. 01-39950 and by the state of Florida. The authors thank D. Robson for helpful discussions.

- [1] E. K. Warburton *et al.*, Phys. Rev. C **41**, 1147 (1990).
- [2] B. V. Pritychenko *et al.*, Phys. Rev. C **63**, 011305 (2001).
- [3] P. D. Cottle and K. W. Kemper, Phys. Rev. C **66**, 061301(R) (2002).
- [4] Y. Utsuno *et al.*, Phys. Rev. C **70**, 044307 (2004).
- [5] G. V. Rogachev *et al.*, Phys. Rev. C **67**, 041603(R) (2003).
- [6] D. J. Millener *et al.*, Phys. Rev. C **28**, 497 (1983).
- [7] D. Guillemaud-Mueller *et al.*, Z. Phys. A **332**, 189 (1989).
- [8] H. Sakurai *et al.*, Phys. Lett. B **448**, 180 (1999).
- [9] A. Arima *et al.*, Phys. Lett. B **24**, 129 (1967).
- [10] A. A. Pilt *et al.*, Phys. Rev. C **19**, 20 (1979).
- [11] S. LaFrance *et al.*, J. Phys. G **5**, L59 (1979).
- [12] K. C. Young *et al.*, Phys. Rev. C **23**, 980 (1981).
- [13] M. Stanoiu *et al.*, Phys. Rev. C **69**, 034312 (2004).
- [14] E. Tryggestad *et al.*, Phys. Rev. C **67**, 064309 (2003).
- [15] S. LaFrance *et al.*, Phys. Rev. C **20**, 1673 (1979).
- [16] E. Khan *et al.*, Phys. Lett. B **490**, 45 (2000).
- [17] D. R. Goosman, Nucl. Instrum. Methods **116**, 445 (1974).
- [18] J. Pavan, Ph.D. dissertation, Florida State University, 2004.
- [19] C. R. Hoffman *et al.*, Phys. Rev. C **68**, 034304 (2003).
- [20] S. Hinds *et al.*, Nucl. Phys. **38**, 81 (1962).
- [21] F. Ajzenberg-Selove, Nucl. Phys. **A300**, 1 (1978).
- [22] F. Ajzenberg-Selove, Nucl. Phys. **A392**, 1 (1983).
- [23] D. H. Gloeckner and R. D. Lawson, Phys. Lett. **53B**, 313 (1974).
- [24] J. B. McGrory and B. H. Wildenthal, Phys. Rev. C **7**, 974 (1973).
- [25] A. Volya and V. Zelevinsky, Phys. Rev. Lett. **94**, 052501 (2005).
- [26] D. Cortina-Gil *et al.*, Phys. Rev. Lett. **93**, 062501 (2004).
- [27] B. A. Brown, Prog. Part. Nucl. Phys. **47**, 517 (2001).
- [28] <http://www.nndc.bnl.gov> (as of November 2004).